Practical Entanglement Estimation for Spin-System Quantum Simulators

O. Marty, M. Cramer, and M. B. Plenio

Practical Entanglement Estimation for Spin-System Quantum Simulators

O. Marty, M. Cramer and M.B. Plenio

Institut für Theoretische Physik & IQST, Albert-Einstein-Allee 11, Universität Ulm, Germany

We present practical methods to measure entanglement for quantum simulators that can be realized with trapped ions, cold atoms, and superconducting qubits. Focussing on long- and short-range Ising-type Hamiltonians, we introduce schemes that are applicable under realistic experimental conditions including mixedness due to, e.g., noise or temperature. In particular, we identify a single observable whose expectation value serves as a lower bound to entanglement and which may be obtained by a simple quantum circuit. As such circuits are not (yet) available for every platform, we investigate the performance of routinely measured observables as quantitative entanglement witnesses. Possible applications include experimental studies of entanglement scaling in critical systems and the reliable benchmarking of quantum simulators.

Introduction—Harnessing the potential of well-controlled experimental platforms, quantum simulators have recently emerged as analogue devices to study paradigmatic condensed-matter models [1]. To date, a considerable variety of devices have been proposed and partially realised to serve the central aim in this field, the preparation and control of quantum states with a number of constituents that is beyond the reach of classical simulations [2]. For the demonstration of genuinely quantum features of these simulators, it is thus of considerable interest to find methods which quantify entanglement and, if possible, relate the findings to classical simulatability. For pure states, the bi-partite block entanglement is a direct figure of merit for the resources required when simulating many-body systems with numerical methods such as the density-matrix renormalization group [3–5]. One way to obtain the entanglement contained in a state in the laboratory would be to perform full quantum state tomography [6] and to compute the entanglement of the reconstructed state. However, this is not only impractical due to the exponential resources required—the proverbial *curse of dimensionality*—but for many reconstruction schemes it may also lead to a systematic overestimation of the true entanglement content [7]. An experimentally feasible and rigorous alternative is to instead rely on lower bounds which may be obtained directly from measured observables [24] and such lower bounds to the entanglement should (i) rely only on a few observables in order to avoid the curse of dimensionality, (ii) avoid assumptions on the state in the laboratory (such as, e.g., symmetries, temperature or an underlying Hamiltonian), and (iii) should be applicable to the experimentally relevant setting of mixed states. Indeed, as has already been demonstrated, (i)-(iii) may be met and entanglement may be quantified from significantly less observables than are required for the knowledge of the full state: E.g., collective observables are capable to detect [8–10] and quantify [11–14] entanglement.

We construct and analyze lower bounds to the bi-partite entanglement of states arising in the quantum simulation of a variety of spin models such as

$$\hat{H} = \sum_{i,j=1}^{N} J_{i,j}\hat{\sigma}_z^i\hat{\sigma}_z^j + B\sum_{i=1}^{N}\hat{\sigma}_x^i, \qquad (1)$$

which have recently been implemented in experiments with trapped ions [15–19], superconducting qubits [20], and ultra-cold atoms [21, 22]. We will consider ground states and their quasi-adiabatic dynamical preparation employing realistic noise models, including decoherence-induced mixedness.

Our aim is to quantify bi-partite block entanglement of one part of the chain vs. the rest relying only on measurements of certain observables $\hat{C}_i$. Denoting experimentally obtained expectation values of these observables by c_i [23], we are thus interested in

$$E_{\min}[\{\hat{C}_i\},\{c_i\}] = \min_{\hat{\varrho}}\left\{E(\hat{\varrho})\,\big|\,\mathrm{tr}[\hat{C}_i\hat{\varrho}] = c_i\right\}, \qquad (2)$$

i.e., we consider the minimal amount of entanglement that is consistent with the obtained measurements c_i. Here, E is the entanglement measure of choice and the minimization is taken over all density matrices $\hat{\varrho}$. As such, we follow the programme initiated in Refs. [24]. Note that no assumption on the state in the laboratory enters our considerations. While we will present tailored lower bounds to $E_{\min}$ that work particularly well—in some cases even providing $E_{\min}$ exactly—for certain classes of states, we stress that all bounds presented in this work are valid for *arbitrary* states – pure or mixed.

For systems governed by Hamiltonians as in Eq. (1), we identify a single key quantity in order to obtain lower bounds on $E_{\min}$. That is, it turns out that a single observable $\hat{C}$ constitutes a common quantitative witness and, in fact, for large classes of states determines not only a lower bound but the entanglement of $\hat{\varrho}$ itself. We show how this witness may be measured directly by employing a simple quantum circuit. If such a circuit is available, entanglement may thus be quantified for systems consisting of an arbitrary number of spins. If it is not available, the above observation still allows us to (i) transform the numerical minimization in Eq. (2) into the problem of computing the smallest eigenvalue of a sparse matrix and thus obtain results for more than 20 spins (and in principle many more using DMRG methods [5]) and (ii) to analytically derive quantitative witnesses that are simple to measure for an arbitrary number of spins, thus avoiding optimisation altogether. With recent implementations of models as in Eq. (1) in mind, we thus introduce schemes for practical and rigorous experimental entanglement estimation using only a few readily available observables and without relying on any as-

sumptions on the state in laboratory.

Throughout, we will use the logarithmic negativity [25] as our bipartite entanglement measure and consider the bipartition $\{1, \ldots, \frac{N}{2}\}|\{\frac{N}{2}+1, \ldots, N\}$, assuming N to be even. The logarithmic negativity is a full entanglement monotone for mixed states [26] and reduces to the Rényi entanglement entropy with Rényi index $1/2$ on pure states.

Preliminaries—We start by introducing the relevant quantities. The logarithmic negativity is defined as

$$E_{\text{l.n.}}(\hat{\varrho}) = \log \|\hat{\varrho}^\Gamma\|_1, \tag{3}$$

where $\hat{\varrho}^\Gamma$ is the partial transpose of $\hat{\varrho}$ with respect to the chosen bipartition and $\|\hat{X}\|_1 = \max\{\text{tr}(\hat{C}\hat{X})\,|\, -\mathbb{1} \leq \hat{C} \leq \mathbb{1}\}$ is the trace norm. By its variational form we have that any observable with $-\mathbb{1} \leq \hat{C}^\Gamma \leq \mathbb{1}$ fulfils $E_{\text{l.n.}}(\hat{\varrho}) \geq \log\langle\hat{C}\rangle_{\hat{\varrho}}$. Any such observable $\hat{C}$ thus serves as a quantitative entanglement witness as it not only witnesses entanglement but indeed provides a lower bound. As an important example for such a quantitative witness consider the un-normalized maximally entangled state $|\Phi\rangle = 2^{N/4}\bigotimes_{i=1}^{N/2}|\phi\rangle_{i,N+1-i}$, where $|\phi\rangle_{i,j} = (|00\rangle + |11\rangle)/\sqrt{2}$, which fulfils $-\mathbb{1} \leq \left(\hat{U}|\Phi\rangle\langle\Phi|\hat{U}^\dagger\right)^\Gamma \leq \mathbb{1}$ for any unitary $\hat{U} = \hat{V} \otimes \hat{W}$. Hence, for any state $\hat{\varrho}$

$$E_{\text{l.n.}}(\hat{\varrho}) \geq \log \max_{\hat{U}=\hat{V}\otimes\hat{W}} \langle\hat{U}|\Phi\rangle\langle\Phi|\hat{U}^\dagger\rangle_{\hat{\varrho}}. \tag{4}$$

The significance of the quantitative witness $\hat{U}|\Phi\rangle\langle\Phi|\hat{U}^\dagger$ becomes clear when considering pure states: For a given pure state, consider its Schmidt decomposition $|\psi\rangle = \sum_s \psi_s|a_s\rangle|b_s\rangle$ and let $\hat{U} = \hat{V} \otimes \hat{W}$ be the unitary that takes $|\Phi\rangle$ to $\sum_s |a_s\rangle|b_s\rangle$. Then $\langle\psi|\hat{U}|\Phi\rangle = \|(|\psi\rangle\langle\psi|)^\Gamma\|_1^{1/2}$ and thus Eq. (4) becomes an equality.

While in general this requires the knowledge of the Schmidt vectors, we will see below that for large classes of states, equality may be achieved for one particularly simple unitary. This fact may be used to greatly simplify the optimization in Eq. (2). Furthermore, for these classes of states, $\langle\hat{U}|\Phi\rangle\langle\Phi|\hat{U}^\dagger\rangle_{\hat{\varrho}}$ may be obtained directly by applying a simple quantum circuit as in Fig. 1b) consisting of mutually commuting $N/2$ two-qubit controlled-not and $N/2$ single-qubit gates and subsequently performing a projective measurement of $|0\rangle\langle0|^{\otimes N}$ in the computational basis.

Results—The Ising model in Eq. (1) has been realized on a variety of experimental platforms: Systems with tunable interactions are for example found in devices based on superconducting qubits [20]. Short-ranged couplings are encountered in experiments with ultra-cold atoms in optical lattices, see, e.g., Ref. [21], in which nearest-neighbour interactions have been simulated. For ion-traps, the implementation of Eq. (1) has been proposed theoretically [28] and realised experimentally [15–17]. Details about $J_{i,j}$ are given in [27]. Often they are well approximated by an algebraic decay,

$$J_{i,j} = \frac{J}{|i-j|^p}, \qquad 0 < p < 3. \tag{5}$$
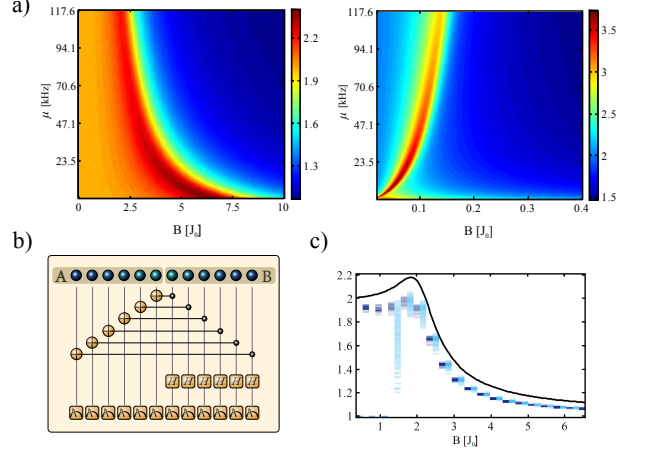

FIG. 1. a) Expectations of $|\Phi\rangle\langle\Phi|$ for the ground state of the ferromagnetic (left) and of $|\Phi'\rangle\langle\Phi'|$ for the ground state of the antiferromagnetic (right) long-range Ising Hamiltonian in Eq. (1) for realistic couplings [27] with $N = 20$ and B in units of $J_0 = \sum_i |J_{i,i+1}|/(N-1)$. The coupling range is determined by the detuning parameter μ. b) The expectations may be obtained via the circuit in Eq. (7) and they coincide with the entanglement in the ground state, see Corollary 1. c) Lower bounds to the entanglement of ground states of the Hamiltonian in Eq. (1) with $N = 16$, $\mu = 117.6$ kHz and realistic couplings [27]. The black line shows the exact logarithmic negativity of the ground state. Entanglement bounds are obtained by optimizing the quantitative witness in Eq. (8) over w_1. The couplings in the witness are as in the Hamiltonian but randomly perturbed by 2% to mimic imprecise knowledge and shown are several random trials as density plots with the optional operator $\bigotimes_{i=1}^N \hat{\sigma}_x^i$ in blue and without in cyan.

Our main result is that for ground states $|\psi\rangle$ of a variety of spin Hamiltonians the maximizing unitary in Eq. (4) may be given explicitly and achieves equality [27]:

$$E_{\text{l.n.}}(|\psi\rangle\langle\psi|) = \log \text{tr}[\hat{U}|\Phi\rangle\langle\Phi|\hat{U}^\dagger|\psi\rangle\langle\psi|]. \tag{6}$$

We prove in [27] that this holds for couplings as in Eq. (5), for all given numerical examples (see Sec. I of [27]), and more general models. Crucially, $\hat{U}$ does *not* depend on the details of the model. Hence, the bipartite entanglement (between the left and right half of the chain as quantified in terms of the logarithmic negativity) of *any* state that is a non-degenerate ground state of a Hamiltonian as in Eq. (1) with couplings fulfilling the hypotheses given in [27] is equal to the expectation value of a simple (unnormalized) projector. What is more, this expectation value serves as a lower bound to the entanglement of *any* state (pure or mixed). One possibility to obtain this expectation value—so the overlap of the state in the laboratory with $|\Phi\rangle$—is to apply a simple circuit and subsequently measuring the projector $|0\rangle\langle0|^{\otimes N}$: For the ferromagnetic case, $(J < 0)$, we write $|\Phi\rangle = \hat{R}^\dagger|0\rangle^{\otimes N}$, where

$$\hat{R} = \bigotimes_{i=1}^{N/2} \hat{H}_i \hat{C}_{i,N+1-i} \tag{7}$$

and $\hat{C}_{i,j}$ denotes the controlled-not gate acting on spin i (control) and j (target) and $\hat{H}_i$ the Hadamard gate acting on spin i. The antiferromagnetic case ($J > 0$) follows by additionally applying the transformation $\bigotimes_{i=1}^{N/2} \hat{\sigma}_x^i$ before the measurement. Note that, e.g., in ion trap experiments, spin polarization measurements along a particular axis are routinely performed by spin-dependent resonance fluorescence.

The logarithmic negativity of any state may thus be lower bounded by applying the circuit $\hat{R}$, which is depicted in Fig. 1b. There, we also show numerical results for the thus obtained entanglement of the ground state of the Ising model in Eq. (1) for realistic [27] ferro- and antiferromagnetic couplings; cf. the phase diagram from the entanglement entropy in Ref. [32].

Although experimentally feasible (see e.g. Ref. [33] for the realization of a CNOT gate in ion traps and Ref. [34] for superconducting qubits), other observables may be more accessible than the implementation of the circuit $\hat{R}$. To this end, we give lower bounds to Eq. (2) in terms of arbitrary observables $\hat{C}_i$. Combining Eqs. (2) and (4), we find that $E_{\min}[\{\hat{C}_i\}, \{c_i\}]$ is lower bounded by the logarithm of $\langle \hat{W} \rangle_{\hat{\varrho}} = \sum_i w_i c_i$ for any operator $\hat{W} := \sum_i w_i \hat{C}_i$ fulfilling $\hat{W} \leq |\Phi\rangle\langle\Phi|$. In particular, an optimal bound may be obtained by optimizing over the w_i using a semidefinite program (SDP) [27]. Note that the observables $\hat{C}_i$ are entirely arbitrary and this scheme thus may accommodate measurements of any experimental platform.

Motivated by the fact that if the ground state is separated from the first excited state by an energy gap, the Hamiltonian itself provides an entanglement witness [38], we consider witnesses of the form

$$\hat{W} = w_0 \mathbb{1} + \bigotimes_{i=1}^{N} \hat{\sigma}_x^i + w_1 \hat{H}, \qquad (8)$$

where we included the (optional, see Fig. 1c) operator $\bigotimes_{i=1}^{N} \hat{\sigma}_x^i$ to account for the small gap in the symmetry-broken phase. This further simplifies the optimization over the variables $\{w_i\}$ as now we are considering only one observable—namely $\hat{W}$—and the number of optimization variables is reduced to one. Note that for $\hat{H}$ as in Eq. (1), the witness $\hat{W}$ consists of at most quadratically many two-body observables and hence its expectation value may in this sense be obtained efficiently: The experimental effort is reduced to obtaining the expectation value of the magnetization $\sum_i \hat{\sigma}_x^i$ and all pairs $\hat{\sigma}_z^i \hat{\sigma}_z^j$ for which $J_{i,j}$ is non-zero. In ion-trap and superconducting-qubit experiments such observables are routinely measured. For nearest-neighbour couplings as, e.g., the ultra-cold atoms experiment in Ref. [21], this amounts to only linearly many observables, the correlators $\hat{\sigma}_z^i \hat{\sigma}_z^{i+1}$ may be obtained directly under a quantum-gas microscope [21], and the magnetization by a Fourier-transformation of the time-of-flight distribution. For the couplings one could either choose a theoretical prediction (for ion traps given in Sec. I of [27]) or, if possible, measure them experimentally (see the methods used in Ref. [18] for ion traps). Then the SDP may be avoided completely by choosing w_0 as the smallest eigen-

value of $|\Phi\rangle\langle\Phi| - \bigotimes_{i=1}^{N} \hat{\sigma}_x^i - w_1 \hat{H}$ as then the constraint $\hat{W} \leq |\Phi\rangle\langle\Phi|$ is automatically fulfilled. As this operator is a sparse matrix, standard eigenvalue solvers allow for system sizes of more than 20 qubits. In fact, since $|\Phi\rangle\langle\Phi|$ possesses a representation as a matrix product operator of bond dimension four, DMRG algorithms may be used to obtain the smallest eigenvalue for much larger systems. In Fig. 1c) we show numerical results for the above procedure. Again, we do not put any assumptions on the state in the laboratory—the expectation $\langle \hat{W} \rangle_{\hat{\varrho}}$ is a lower bound to the entanglement of any state $\hat{\varrho}$ but, of course, we know that the bound will work particularly well for ground states of Hamiltonians as in Eq. (1) with couplings as in Eq. (5) or as in Sec. I of [27] with parameters as for all the numerical examples considered here. Finally we use the condition $\hat{W} \leq |\Phi\rangle\langle\Phi|$ to determine a witness $\hat{W}$ (see [27] for details) in terms of observables which are readily measurable with trapped ions. Notably, $\hat{W}$ allows for lower bounds for ground states of Hamiltonians as in Eq. (1) independent of the magnetic field, see Fig. 2. With this quantitative witness one is hence in the position of directly giving lower bounds by obtaining expectation values of simple operators and neither the implementation of a circuit nor optimisation is necessary, which allows for the application to an arbitrary number of spins.

Quasi-adiabatic preparation and benchmarking—In non-equilibrium situations, quantum simulators of one-dimensional spin systems may outperform classical computers already for a moderate size of spins: As opposed to states in equilibrium, which typically have little entanglement (cf., *area laws* for ground and thermal states [3, 41]), the entanglement generated in non-equilibrium situations may become large [42]. Arguably the best numerical algorithms for the simulation of one-dimensional (non-)equilibrium quantum many-body systems are those based on matrix product states (MPS) and matrix product operators (MPO) [5, 43]. The resources required to treat such states numerically are directly related to their so-called *bond dimension*. For pure states, i.e. MPS, there is an intimate relation between the bond dimension and the entanglement content as quantified in terms of Rényi entanglement entropies [4]. For mixed states, i.e. MPO, this connection is far less clear. Indeed, an MPO may have a small bond dimension while at the same time have a large block entropy—the product operator $(\mathbb{1}/2)^{\otimes N}$ being the most striking example. In this sense, using pure-state entanglement measures (such as Rényi entanglement entropies) as benchmarks may lead to false conclusions because in experiments mixedness is unavoidable. We illustrate these relations by considering the quasi-adiabatic preparation of ground states of Ising Hamiltonians as commonly performed in ion-trap experiments [17, 27]. Numerical results are summarized in Fig. 2 The main conclusions are: The block entropy $S(\mathrm{tr}_{1,\ldots,N/2}[\hat{\varrho}(t)])$ (a measure of entanglement if the state was pure) increases with time for all noise-strengths while the true entanglement reaches a maximum after which it decreases in time. From the block entropy one would thus falsely conclude that the state becomes harder and harder to
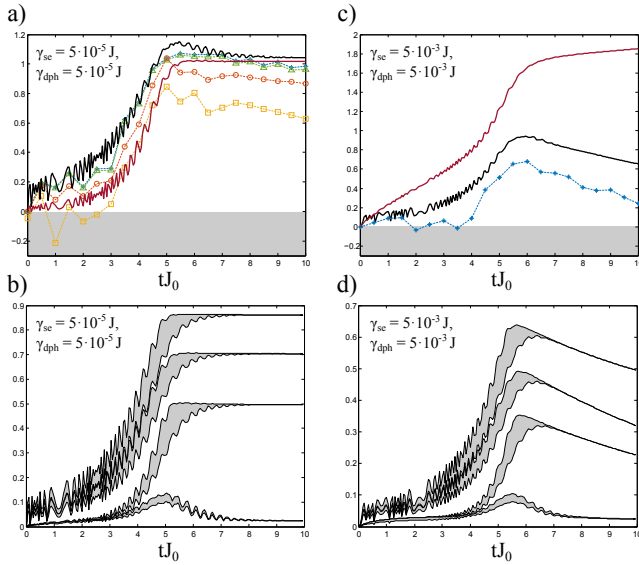
FIG. 2. Quasi-adiabatic ramping of the magnetic field across the phase transition including spontaneous emission and dephasing simulated using a Lindblad model [27] for $N = 8$ spins, leading to a relatively long-ranged interaction $\sim |i - j|^{-0.3}$. a), c) Shown are the block entropy $S(\mathrm{tr}_{1,...,N/2}[\hat{\varrho}(t)])$ (an entanglement measure if the state was pure) in red, the exact bi-partite entanglement of the simulated state $\hat{\varrho}(t)$ in black, lower bounds as obtained by the circuit $\hat{R}$ (blue crosses), by the witness Eq. (S35) in [27] (green triangles), by the SDP [27] with observables $\hat{\sigma}_\alpha^i$, $\hat{\sigma}_\alpha^i\hat{\sigma}_\alpha^j$, $i, j = 1, \dots, N$, $\alpha = x, y, z$, and $\hat{\sigma}_x^1 \cdots \hat{\sigma}_x^N$ as input (orange circles), and by optimizing the quantitative witness in Eq. (8) over w_1 and B (yellow squares). See [27] for a detailed noise analysis. b), d) Shown in grey are upper and lower bounds [44] to the MPO approximation error in Eq. (9) ($D = 1, 2, 3, 4$ top to bottom). Note the monotonicity of the block entropy as opposed to the behaviour of the approximation error and the entanglement as quantified in terms of the logarithmic negativity.

simulate while the error when approximating $\hat{\varrho}(t)$ by an MPO $\hat{\varrho}_D$ with bond dimension D,

$$\epsilon_D(t) = \min_{\hat{\varrho}_D} \|\hat{\varrho}(t) - \hat{\varrho}_D\|_F, \qquad (9)$$

reaches a maximum and then decreases in time [44] as does the entanglement. The exact mathematical connection between approximability by MPOs, entanglement, and other quantities such as, e.g., mutual information, remains an open question however.

Summary and Outlook—In the setting of quantum simulations of the transverse- field Ising model, we have introduced methods to estimate bi-partite block entanglement without putting any assumptions on the state in the laboratory. The principles presented here are applicable to, e.g., ion-trap, cold-gases, and superconducting-qubit implementations and we have focused on the ion-trap platform for specific examples. A lower bound to the entanglement is given by the overlap with a certain state, which may, e.g., be obtained by a simple quantum circuit and, for large classes of states, actually gives the entanglement exactly instead of just bounding it. As obtain-

ing this overlap may, depending on the platform, may represent a considerable experimental challenge, we further investigated the performance of routinely performed measurements as means to estimate the entanglement. As we consider the benchmarking of quantum simulators as one possible application, we have compared the matrix-product-operator bond dimension, block entanglement, and block entropy for a quasi-adiabatic protocol preparing ground states of the transverse-field Ising model.

[1] T.H. Johnston, S.R. Clark and D. Jaksch, *EPJ Quant. Tech.* **1**:10 (2014).

[2] I.M. Georgescu, S. Ashhab, F. Nori, *Rev. Mod. Phys.* **86**, 153 (2014).

[3] J. Eisert, M. Cramer, M.B. Plenio, *Rev. Mod. Phys.* **82**, 277 (2010).

[4] N. Schuch, M.M. Wolf, F. Verstraete and J.I. Cirac, *Phys. Rev. Lett.* **100**, 030504 (2008).

[5] U. Schollwöck, *Rev. Mod. Phys.* **77** 259 (2005); U. Schollwöck, *Ann. of Phys.* **326** (1), 96 (2011).

[6] M. Paris, J. Rehacek, Quantum State Estimation, *Lecture Notes in Physics*, 649 (Springer, Heidelberg, 2004); K. Banaszek, M. Cramer, and D. Gross, *New J. Phys.* **15**, 125020 (2013).

[7] C. Schwemmer, L. Knips, D. Richart, T. Moroder, M. Kleinmann, O. Gühne, and H. Weinfurter, *Phys. Rev. Lett.* **114**, 080403 (2015).

[8] M. Wieśniak, V. Vedral and Č. Brukner, *New J. of Phys.* **7**, 258 (2005).

[9] G. Tóth, C. Knapp, O. Gühne and H.J. Briegel, *Phys. Rev. Lett.* **99**, 250405 (2007).

[10] P. Krammer, H. Kampermann, D. Bruss, R.A. Bertlmann, L.C. Kwek, and C. Macchiavello, *Phys. Rev. Lett.* **103**, 100502 (2009).

[11] M. Cramer, M.B. Plenio and H. Wunderlich, *Phys. Rev. Lett.* **106**, 020401 (2011).

[12] O. Marty, M. Epping, H. Kampermann, D. Bruß, M.B. Plenio, and M. Cramer, *Phys. Rev. B* **89**, 125117 (2014).

[13] M. Cramer, A. Bernard, N. Fabbri, L. Fallani, C. Fort, S. Rosi, F. Caruso, M. Inguscio, and M.B. Plenio, *Nat. Commun.* **4**, 2161 (2013).

[14] B. Lücke, J. Peise, G. Vitagliano, J. Arlt, L. Santos, G. Tóth and C. Klempt, *Phys. Rev. Lett.* **112**, 155304 (2014).

[15] A. Friedenauer, H. Schmitz, J.T. Glueckert, D. Porras, and T. Schaetz, *Nat. Phys.* **4**, 757 (2008).

[16] K. Kim, M.-S. Chang, S. Korenblit, R. Islam, E.E. Edwards, J.K. Freericks, G.-D. Lin, L.-M. Duan and C. Monroe, *Nature* **465**, 590 (2010).

[17] R. Islam, E.E. Edwards, K. Kim, S. Korenblit, C. Noh, H. Carmicheal, G.-D. Lin, L.-M. Duan, C.-C. Joseph Wang, J.K.

Freericks and C. Monroe, *Nat. Comm.* **2**, 377 (2011).

[18] P. Jurcevic, B.P. Lanyon, P. Hauke, C. Hempel, P. Zoller, R. Blatt, C.F. Roos, *Nature* **511**, 202 (2014).

[19] P. Richerme, Z.-X. Gong, A. Lee, C. Senko, J. Smith, M. Foss-Feig, S. Michalakis, A.V. Gorshkov, and C. Monroe, *Nature* **511**, 198 (2014).

[20] M.W. Johnson, et al., *Nature* **473**, 194 (2011); S. Boixo, T. Albash, F.M. Spedalieri, N. Chancellor, and D.A. Lidar, *Nat. Comm.* **4**, 3067 (2013); S. Boixo, T.F. Rønnow, S.V. Isakov, Z. Wang, D. Wecker, D.A. Lidar, J.M. Martinis and M. Troyer, *Nature Physics* **10**, 218 (2014).

[21] J. Simon, W.S. Bakr, R. Ma, M.E. Tai, P.M. Preiss and M. Greiner, *Nature*, **472**, 307 (2011).

[22] F. Meinert, M.J. Mark, E. Kirilov, K. Lauber, P. Weinmann, A.J. Daley, and H.-C. Nägerl, *Phys. Rev. Lett.* **111**, 053003 (2013).

[23] Of course, in an experimental scenario, expectation values can never be obtained exactly and one needs to incorporate such errors into the theory. One way is to, instead of equality in Eq. (2), consider $|\mathrm{tr}[\hat{C}_i \hat{\varrho}] - c_i| \leq \epsilon_i$ along with a certain confidence and propagate these errors through the minimization, assigning a corresponding confidence to the minimal entanglement $E_{\min}$. Most of our results however are lower bounds to $E_{\min}$ that take the form of a single expectation value $\mathrm{tr}[\hat{C}\hat{\varrho}]$ such that the usual error estimates for obtaining mean values apply.

[24] R. Horodecki, M. Horodecki, and P. Horodecki, *Phys. Rev. A* **59**, 1799 (1999); F.G.S.L. Brandão, *Phys. Rev. A* **72**, 022310 (2005); K.M.R. Audenaert and M.B. Plenio, *New J. of Phys.* **8**, 266 (2006); J. Eisert, F.G.S.L. Brandão, and K.M.R. Audenaert, *New J. of Phys.* **9**, 46 (2007); O. Gühne, M. Reimpell, and R.F. Werner, *Phys. Rev. Lett.* **98**, 110502 (2007); O. Gühne, M. Reimpell, and R.F. Werner, *Phys. Rev. A* **77**, 052317 (2008).

[25] M.B. Plenio and S. Virmani, *Quant. Inf. Comput.* **7**, 1 (2007).

[26] M.B. Plenio, *Phys. Rev. Lett.* **95**, 090503 (2005), see Erratum *Phys. Rev. Lett.* **95**, 119902 (2005).

[27] See Supplemental Material.

[28] D. Porras and J.I. Cirac, *Phys. Rev. Lett.* **92**, 207901 (2004).

[29] K. Kim, M.-S. Chang, R. Islam, S. Korenblit, L.-M. Duan and C. Monroe, *Phys. Rev. Lett.* **103**, 120502 (2009).

[30] R. Islam, C. Senko, W.C. Campbell, S. Korenblit, J. Smith, A. Lee, E.E. Edwards, C.-C.J. Wang, J.K. Freericks, C. Monroe, *Science* **340**, 583 (2013).

[31] J. Schachenmayer, B.P. Lanyon, C.F. Roos, A.J. Daley, *Phys. Rev. X* **3**, 031015 (2013).

[32] T. Koffel, M. Lewenstein and L. Tagliacozzo, *Phys. Rev. Lett.* **109**, 267203 (2012).

[33] M. Riebe, T. Monz, A. S. Villar, P. Schindler, M. Chwalla, M. Hennrich and R. Blatt, *Nat. Phys.* **4**, 839 (2008); P. Schindler, D. Nigg, T. Monz, J.T. Barreiro, E. Martinez, S.X. Wang, S. Quint, M.F. Brandl, V. Nebendahl, C.F. Roos, M. Chwalla, M. Hennrich, and R. Blatt, *New J. Phys.* **15**, 123012 (2013).

[34] J.H. Plantenberg, P.C. de Groot, C.J. P.M. Harmans, and J.E. Mooij, *Nature* **447** 836 (2007); J.M. Chow, J.M. Gambetta, A.D. Córcoles, S.T. Merkel, J.A. Smolin, C. Rigetti, S. Poletto, G.A. Keefe, M.B. Rothwell, J.R. Rozen, M.B. Ketchen, and M. Steffen, *Phys. Rev. Lett.* **109**, 060501 (2012).

[35] J.F. Sturm, *Opt. Meth. Soft.* **11**, 625 (1999).

[36] X. Sao, D. Sun, K.-J. Toh, *SIAM J. Opt.* **20**, 1737 (2010).

[37] Z. Wen, D. Goldfarb, W. Yin, *Math. Prog. Comp.* **2**, 203 (2010).

[38] In fact, for ground states $|\psi\rangle$ of (1) with energy gap Δ, one has, for any state $\hat{\varrho}$, that $\|\hat{\varrho}^\Gamma\|_1 \geq \||\psi\rangle\langle\psi|^\Gamma\|_1 - 2(2^N\langle\hat{H}\rangle_{\hat{\varrho}}/\Delta)^{1/2}$. See also Refs. [39, 40].

[39] M.R. Dowling, A.C. Doherty and S.D. Bartlett, *Phys. Rev. A* **70**, 062113 (2004).

[40] O. Gühne, G. Tóth and H.J. Briegel, *New J. of Phys.* **7**, 229 (2005).

[41] K.M.R. Audenaert, J. Eisert, M.B. Plenio, and R.F. Werner, *Phys. Rev. A* **66**, 042327 (2002); M.B. Plenio, J. Eisert, J. Dreißig, and M. Cramer, *Phys. Rev. Lett.* **94**, 060503 (2005); M.B. Hastings, *Phys. Rev. B* **73**, 085115 (2006); M.B. Hastings, *JSTAT*, P08024 (2007); F.G.S.L. Brandão and M. Horodecki, *Nat. Phys.* **9**, 721 (2013); M. Kliesch, C. Gogolin, M.J. Kastoryano, A. Riera, and J. Eisert, *Phys. Rev. X* **4**, 031019 (2014); F.G.S.L. Brandão and M. Horodecki, *Comm. Math. Phys.* **333**, 761 (2015).

[42] S. Bravyi, M.B. Hastings, and F. Verstraete, *Phys. Rev. Lett.* **97**, 050401 (2006); J. Eisert and T.J. Osborne, *Phys. Rev. Lett.* **97**, 150404 (2006).

[43] M. Fannes, B. Nachtergaele, and R.F. Werner, *Comm. Math. Phys.* **144**, 443 (1992); D. Perez-Garcia, F. Verstraete, M.M. Wolf, and J.I. Cirac, *Quant. Inf. Comp.* **7**, 401 (2007); V. Murg, J.I. Cirac, B. Pirvu, and F. Verstraete, *New J. Phys.* **12**, 025012 (2010).

[44] $\|\cdot\|_F$ denotes the Frobenius norm and the minimization is over MPOs with bond dimension D. In Fig. 2 we show lower and upper bounds to this quantity. The upper bound is obtained using a variational compression method described in [5] and the lower bound may be obtained directly from the state $\hat{\varrho}(t)$ by considering its coefficient matrix: One has $\epsilon_D(t)^2 \geq \max_l \sum_{i>D} \lambda_i^{(l)2}$, where $\lambda_i^{(l)}$ denote the operator Schmidt-coefficients of $\hat{\varrho}(t)$ with respect to the bipartition $\{1, \ldots, l\}\{l+1, \ldots, N\}$ in decreasing order.

[45] R. Horn, *Trans. Amer. Math. Soc.* **136**, 269-286 (1969).

[46] F. Hiai, *Lin. Alg. Appl.* **431**, 1125-1146 (2009).

[47] F.D.M. Haldane, *Phys. Rev. Lett.* **50**, 1153 (1983).

[48] I. Affleck, *J. Phys: Condens. Matter.* **1**, 3047 (1989).

[49] C. Li, J. Fan, L. Yu, G. Chen, T.-C. Zhang, and S. Jia, E-print arXiv:1502:00470 (2015).

[50] I. Affleck, and E.H. Lieb *Lett. Math. Phys.* **12**, 57 (1986).

[51] E.J. Candès, M.B. Walkin and S.P. Boyd *J. Four. Anal. Appl.* **14**(5), 877 (2008).

[52] M. Huber, and R. Sengupta *Phys. Rev. Lett.* **113**, 100501 (2014).